Modeling studies of dust/gas non-thermal equilibrium in the Martian atmosphere.

R.M. Haberle*, **M.A. Kahre,** *NASA Ames Research Center, Moffett Field CA, USA,* **T. Bertrand,** *LESIA Observatoire de Paris, MEUDON, France,* **V.L. Hartwick**, **R.J. Wilson**, *NASA Ames Research Center, Moffett Field CA, USA,* **M. Wolff**, *Space Science Institute, Boulder, CO. USA,* **C. Batterson**, *Bay Area Environmental Research Institute, Moffett Field CA, USA.* ***** Retired Jan 4, 2022 (rmhaberle@sbcglobal.net)

Introduction: Heating rate calculations of the Martian atmosphere generally assume that collisional interactions between dust particles and gas molecules maintain a thermal equilibrium in which both have the same temperature. However, above 40 km Goldenson et al. (2008) show that collisional interactions are unable to maintain this equilibrium and that dust and gas temperatures diverge with differences approaching 50 K or more depending mostly on particle size and altitude. Since observations (e.g., Sanchez-Lavega et al. 2018; Heavens et al. 2019) and modeling studies (e.g., Bertrand et al., 2020; Batterson et al., 2021; 2022, this meeting) show that dust can reach altitudes well above 40 km, and since heating rates drive atmospheric circulation systems, it is worth assessing the magnitude of non-equilibrium conditions on the thermal structure and dynamics of the Martian atmosphere.
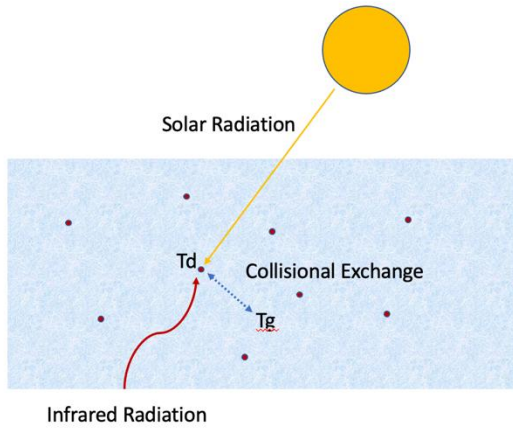
Fig 1. Physics of collisional coupling between dust and gas.

Basic Physics: The cartoon depicted in Figure 1 illustrates the situation. The total radiative heating of a given atmospheric layer is due to the net flux divergence of solar and infrared radiation. These fluxes are readily calculated, for example, from two-stream solutions to the radiative transfer equation that account for gaseous absorption and multiple scattering (e.g., Mischna et al. 2012). In a mixed system with both dust particles and gas molecules the total heating of a given layer is partitioned between dust and gas. In the case where collisional coupling between dust and gas is strong, as in the lower Martian atmosphere, dust and gas will have the same temperature, thermal equilibrium is maintained, and the net flux divergence heats the layer uniformly. However, in the absence of strong collisional coupling, as at high altitudes in the Martian atmosphere, thermal contact is lost, dust and gas temperatures differ, thermal equilibrium is not maintained, and the layer heats non-uniformly.

Methodology: We begin our study with a 1-D time marching radiative-convective model then implement the routines into our NOAA/GFDL cubed-sphere finite volume (FV3-based) GCM (see Kahre et al., 2022; this meeting). The model radiative routines are described in Haberle et al. (2019). Two changes are needed to implement the physics described above into the 1D and FV3-based models: incorporating an algorithm to compute dust particle temperatures and modifying the Planck function to account for the difference in temperature between dust and gas.
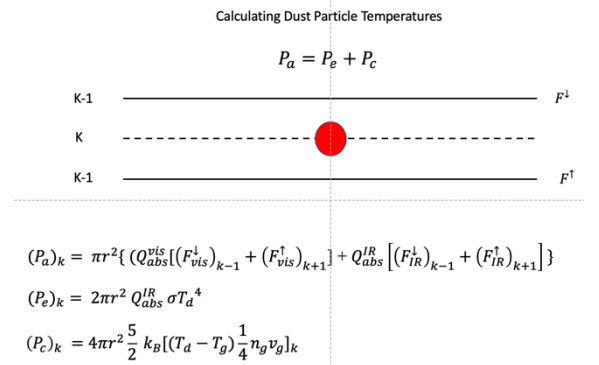
Fig 2. At a given level k, an iterative solution is used to solve for the dust particle temperature T_d in terms particle size r, absorption efficiency Q_{abs}, upward and downward fluxes $F^\uparrow$ and $F^\downarrow$, gas temperature T_g, and gas kinetic theory coefficients, k_b, v_g, n_g.

Dust Particle Temperatures. We follow the methods of Goldenson et al. (2008) which are based on those of Fiocco et al. (1975). As illustrated in Figure 2, the power of absorbed solar and infrared radiation (P_a) is assumed to be balanced by emission (P_e) and collisional (P_c) losses. The terms in the power equation depend on particle size, absorption efficiencies, the fluxes incident on the particle, and several coefficients based on gas kinetic theory. In the modeling simulations presented here the fluxes and absorption efficiencies are based on scattering

properties derived from Mie theory assuming a fixed log-normal particle size distribution with an effective radius and variance of 1.5 μm and 0.5, respectively. An iterative solution of the power equation yields the dust particle temperature.

Modified Planck Function. We define the non-equilibrium source function in terms of a weighted mean Planck function, B_w, where the weighting depends on the Planck function at the temperature of the dust (B_d) and gas (B_g), and on layer absorption opacities of the dust (τ_a^d) and gas (τ_a^g). This weighted mean replaces the standard source function in the radiation code. Figure 3 shows the derivation.

Planck Function

The standard Source function within a given spectral interval is

$$S = 2\pi(1 - \omega_o)B$$

A non-equilibrium Source function within a given spectral interval for a single particle size would be

$$S_{ne} = 2\pi(1 - \omega_o)B_w$$

where

$$B_w = \frac{1}{\tau_a^g + \tau_a^d} \left(\tau_a^g B_g + \tau_a^d B_d\right)$$

and

τ_a^g = *gas absorption optical depth*
τ_a^d = *dust absorption optical depth*
B_g = *Planck function at gas temperature*
B_d = *Planck function at dust particle temperature*

Fig 3. Modification of the Planck Function.

1D Simulations: *Run Parameters.* With these modifications we run the model for 10 sols, first with a fixed local time (3 pm) to understand the basic effect, and then over a full diurnal cycle to assess day/night differences and how diurnal amplitudes are modified. Dust temperatures are for 1.5 μm particles.

Steady State Solutions. Results for a typical case are shown in Figure 4. In this simulation the dust is uniformly mixed with a column optical depth of one.

Temperature Profiles
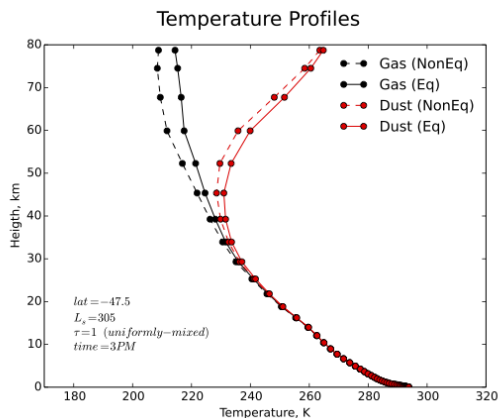
Fig 4. Steady state 3pm temperature profiles of 1.5 μm dust particles (red lines) and gas molecules (black lines) at 47.5°S and L_s 305°. Solid lines use the standard Source function; dashed lines use the non-equilibrium Source function.

As can be seen afternoon dust and gas temperatures begin to diverge above 40 km. Near the model top the difference approaches 70 K. Warmer dust particles increase layer emission and consequently the gas cools. In this case the cooling is on the order of 10 K at 70 km. Thus, loss of thermal contact means a cooler gas temperature and lower static stability in the upper atmosphere.

Diurnal Variations. This result holds for the full diurnal cycle as is illustrated in Figure 5.

Diurnal Temperature Profiles
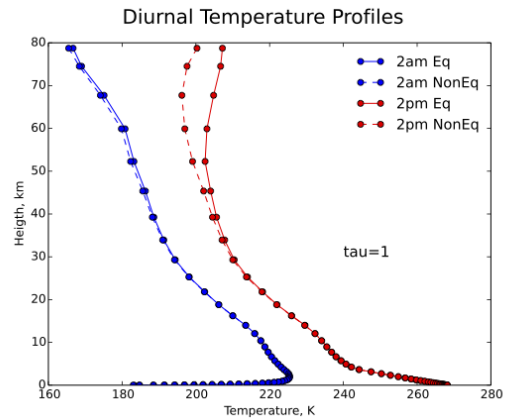
Fig 5. 2pm (red) and 2am (blue) temperature profiles for equilibrium cases (solid lines) and non-equilibrium cases (dashed lines).

Non-equilibrium gas temperature profiles are cooler than the equilibrium profiles, but the difference is greatest for daytime conditions where solar heating is much more effective at raising particle temperatures than infrared heating. This is further illustrated in Figure 6 which also shows that the dust/gas temperature difference increases with altitude as thermal contact weakens.

Dust-Gas Temerature Differences
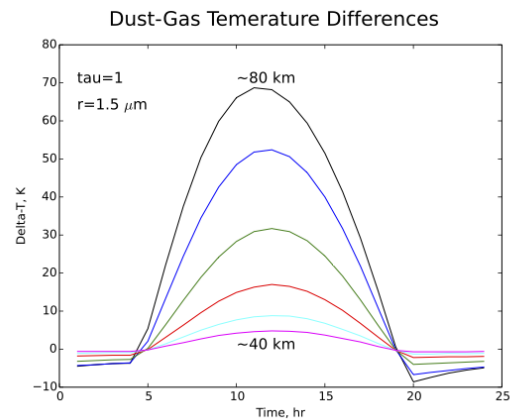
Fig 6. Diurnal variation of the difference between dust particle and gas temperature at several altitudes.

The change in gas temperatures as a function of time of day and altitude when non-equilibrium conditions are included is shown in Figure 7. At all altitudes and all times of day gas temperatures cool. The cooling is modest at low levels (40 km) but increases with altitude. There is a noticeable diurnal variation in the cooling whose amplitude increases with altitude and whose phase gradually shifts from a late afternoon maximum at low altitudes to near

midday at the highest model level (80 km). Though the amplitude is less than 10 K, this change in the gas diurnal temperature behavior at higher altitudes could affect the low-latitude vertically propagating diurnal thermal tide during dusty periods.
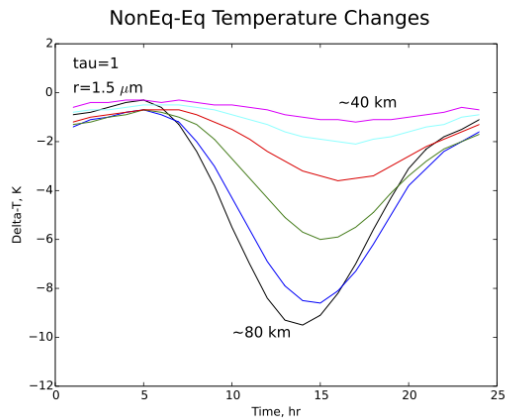
Fig 7. Diurnal variation of the change in gas temperatures when non-equilibrium conditions are included.

GCM Simulations: *Run Parameters*. We have implemented the physics of dust/gas non-thermal equilibrium into our FV3-based GCM and have carried out some preliminary experiments to assess its effect. The results we show are from annual simulations that track a temporal and spatially varying dust opacity map based on Mars Year 34 which has a global dust storm that peaks around L_s 210°. For simplicity, the dust vertical distribution is prescribed using the classical Conrath (1975) prescription with a temporal and spatially constant ν=0.007 which confines most - but not all - of the dust below 50 km. We carry out two simulations: one with dynamics switched off and the one with dynamics switched on. These simulations allow us to assess the influence of heating or cooling by atmospheric motions on the thermal structure and basic wind fields.

Results. As shown in Figure 8 dynamical processes can significantly affect the dust-gas temperature difference.
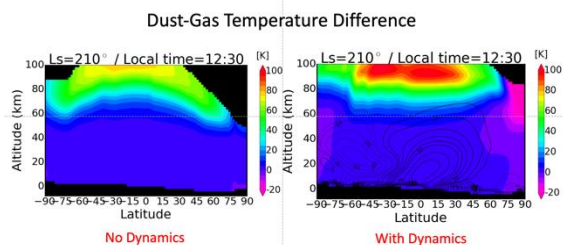
Fig 8. Zonal mean temperature difference between dust and gas for simulations with and without dynamics. Black contours for the "With Dynamics" simulation represent mass stream function in units of 10^8 Kg s^{-1}.

Without dynamics dust particles near the model top at the peak of the dust storm are ~70 K warmer than the gas; with dynamics the difference increases

to ~100 K. At these altitudes dust particle temperatures are largely set by radiative processes which are similar in the two cases. It is therefore likely that this change in dust-gas temperature difference is mostly due to cooler gas temperatures that develop when dynamical processes are included. The thermal tide can have a significant effect on diurnal temperature variations and could account for this behavior.

Perhaps a more interesting question is how non-equilibrium physics might affect global circulation systems. We have just begun our analysis of this question and hope to offer a more complete assessment at the meeting. However, some intriguing changes can be noted.
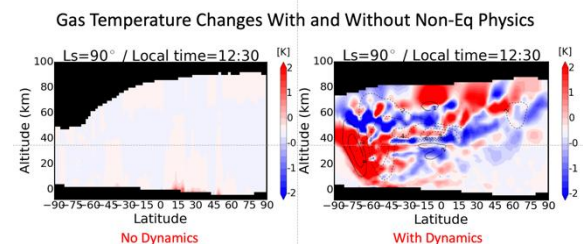
Fig 9. Change in gas temperature when non-equilibrium conditions are imposed. Black contours for the "With Dynamics" case represent changes in the zonal mean zonal wind (m s^{-1}).

The change in gas temperature for simulations with and without the non-equilibrium physics at northern summer solstice is shown in Figure 9. Without dynamics the change is very small (<1K), which is because the dust loading is minimal and confined to low levels. With dynamics, however, the change is larger (up to ~ 5 K) and has a clearly defined pattern. The gas warms throughout the atmosphere below 50 km at high southern latitudes and the poleward tilt of the warming suggests a stronger Hadley circulation. This is confirmed from an analysis of the stream function field and is supported by the strengthening of the zonal winds.

A similar pattern can also be seen at L_s 210° during the peak of the global dust storm (Figure 10).
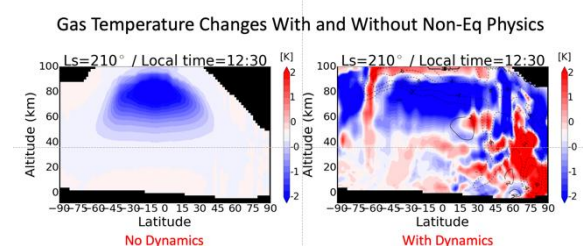
Fig 10. Same as Figure 9 but for L_s=210°.

In this case there is considerable cooling in the upper tropical atmosphere in the absence of dynamics that is largely unmodified by dynamical processes. This is different from the solstice case because the dust loading is much higher and even though it is

still confined to low altitudes its abundance in the upper atmosphere has increased. The warming at high northern latitudes at L_s 210° also appears to be the result of adiabatic warming in the descending branch of a stronger Hadley Cell. The pattern is somewhat more complicated, however, and will require further analysis to fully understand. Nevertheless, it is clear that non-equilibrium physics does have an impact on global circulation systems.

Conclusions: We have shown that loss of thermal contact between dust and gas in the Martian atmosphere occurs above 40 km, confirming the earlier results of Goldenson et al. (2008). Above 40 km, the difference between dust and gas temperature increases with altitude and can be as high as 100 K at 80 km. Because the radiative energy absorbed by dust particles is radiated to space rather than transferred to the gas by collisions, gas temperatures at these levels cool when non-equilibrium conditions are included. The amount of cooling depends on the dust abundance and optical properties but can be on the order of 10 K or so at very high altitudes. Thus, in general, loss of thermal contact means a lower static stability in the upper levels of a deeply dusty atmosphere than equilibrium models would predict.

We have just begun to explore the effect of these changes with our FV3-based GCM and do see changes to global wind fields. In simulations where we have specified the dust vertical distribution, the Hadley circulation and polar jets are altered. It is highly likely that further analysis will show that the thermal tides and other wave motions are also affected. However, we cannot yet say just how important non-equilibrium physics is to these wind systems, the evolution of dust storms, or on the Martian climate system in general. Much more work is needed including careful analyses of well-posed fully interactive simulations. What we can say is that this is a real process that has been ignored by the GCM modeling community (our group included) and since dust is observed to reach very high altitudes, and since we know how to implement the physics into our models, now is a good time to fully explore the consequences of non-equilibrium physics on the thermal structure and wind systems of the Martian atmosphere.

References: Batterson et al. (2021), Fall AGU Meeting, Abstract No. P32C-06. Batterson et al. (2022), 7th MAMO. Bertrand et al. (2020), J. Geophys. Res., 125, doi:10.1029/2019JE006122. Conrath (1975), Icarus, 24, 36-46. Fiocco et al. (1975), J. Atmos. and Terres. Phys., 37, 1327-1337. Goldenson et al. (2008), GRL, 35, doi:10.1029/2007GL-32907. Haberle et al. (2019), Icarus, 333, 130-164. Heavens et al. (2019), J. Geophys. Res., Planets, 124, doi:10.1029/2019JE006110. Mischna et al. (2012), J. Geophys. Res., 113, E10009. Sanchez-Lavega et al. (2018), Icarus, 299, 194-205.